J|A|C|S
ARTICLES
Published on Web 06/24/2004

Double Geminal C−H Activation and Reversible α-Elimination in 2-Aminopyridine Iridium(III) Complexes: The Role of Hydrides and Solvent in Flattening the Free Energy Surface

Eric Clot,[‡] Junyi Chen,[†] Dong-Heon Lee,[§] So Young Sung,[§] Leah N. Appelhans,[†] Jack W. Faller,*[,†] Robert H. Crabtree,*[,†] and Odile Eisenstein*[,‡]

Contribution from the Sterling Chemistry Laboratory, Yale University, New Haven, Connecticut 06520-810; LSDSMS, UMR 5636, Université Montpellier 2, 34095 Montpellier Cedex 5, France; and Department of Chemistry, Chonbuk National University, Chonju, 561-756, Korea

Received March 17, 2004; E-mail: jack.faller@yale.edu; robert.crabtree@yale.edu; odile.eisenstein@univ-montp2.fr

Abstract: $[H_2Ir(OCMe_2)_2L_2]BF_4$ (**1**) (L = PPh_3), a preferred catalyst for tritiation of pharmaceuticals, reacts with model substrate 2-(dimethylamino)pyridine (py-NMe_2; py = 2-pyridyl) to give chelate carbene $[H_2Ir(py\text{-}N(Me)CH{=})L_2]BF_4$ (**2a**) via cyclometalation, H_2 loss, and reversible α-elimination. Agostic intermediate $[H_2Ir(py\text{-}N(Me)CH_2{-}H)L_2]BF_4$ (**4a**), seen by NMR, is predicted (DFT(B3PW91) computations) to give C−H oxidative addition to form the alkyl intermediate $[(H)(\eta^2\text{-}H_2)Ir(py\text{-}N(Me)CH_2{-})L_2]BF_4$. Loss of H_2 leads to the fully characterized alkyl $[HIr(OCMe_2)(py\text{-}N(Me)CH_2{-})L_2]BF_4$ (**3a**^{Me_2CO}), which loses acetone to give alkylidene hydride **2a** by rapid reversible α-elimination. **2a** rapidly reacts with excess H_2 in d_6-acetone to generate $[H_2Ir(OC(CD_3)_2)_2L_2]BF_4$ (**1**-d_{12}), **3a**$^{(CD_3)_2CO}$, and py-NMe_2 in a 1:1:1 ratio, showing reversibility and accounting for the selective isotope exchange catalyzed by **1**. Reaction of **1** with py-$N(CH_2)_4$ gives the fully characterized carbene **2c**. A *cis*-L_2 carbene intermediate, ***cis*-2c**, observed by NMR, reacts with CO via retro α-elimination to give the alkyl **3c**^{CO}, while the trans isomer, **2c**, does not react; retro α-elimination thus requires the Ir−H bond to be orthogonal to the carbene plane. Consistent with experiment, computational studies show a particularly flat PE surface with activation of the agostic C−H bond giving a less stable H_2 complex, then formation of a kinetic carbene complex with *cis*-L, only seen experimentally for py-$N(CH_2)_4$. Hydrides at key positions, together with gain or loss of solvent and H_2, flatten the PE (ΔG) surfaces to allow fast catalysis.

Introduction

$[H_2Ir(OCMe_2)_2L_2]BF_4$ (**1**) (L = PPh_3), or its precursor $[Ir(cod)L_2]BF_4$, is a preferred catalyst for the commercial tritiation of pharmaceuticals.[1,2] A reversible cyclometalation involving coordination at a substrate lone pair and oxidative addition of an adjacent C−H bond with reversible transfer of the CH hydrogen to the metal is thought to be responsible for the selectivity.[3] We now find that where the key substrate CH is activated by an adjacent aliphatic nitrogen, as in 2-(dimethylamino)pyridine (py-NMe_2; py = 2-pyridyl), stoichiometric reaction with **1** leads to transfer of two hydrogens to the metal with loss of H_2 and formation of a carbene complex. The presence of this normally very stable species might be expected to slow the isotope exchange by making the H transfers less easily reversible. Experimentally, rapid isotope exchange still occurs, however. DFT calculations show that the presence of hydrides at key positions in the catalyst intermediates together with gain or loss of solvent and H_2 flatten the Gibbs free energy surfaces to allow fast reversible α-hydride elimination and isotope exchange in this system. A preliminary report has appeared on a small part of this work (Scheme 1).[4]

Unlike reversible β-hydride elimination, well studied in catalytic reactions such as olefin isomerization, reversible α-hydride elimination is rare. Evidence for an equilibrium between an alkyl complex and alkylidene hydride has generally involved high oxidation state early transition metal complexes, notably of tungsten[5−9] and tantalum.[10−14] An equilibrium between $Cp^*_2Ta(=CH_2)(H)$ and the unobservable $Cp^*_2Ta{-}CH_3$

[†] Yale University.
[‡] Université Montpellier 2.
[§] Chonbuk National University.

(1) Saljoughian, M.; Williams, P. G. *Curr. Pharm. Des.* **2000**, *6*, 1029.
(2) Shu, A. Y. L.; Saunders, D.; Levinson, S. M.; Landwatter, S. W.; Mahoney, A.; Senderoff, S. G.; Mack, J. F.; Heys, J. R. *J. Labelled Compd. Radiopharm.* **1999**, *42*, 797.
(3) Crabtree, R. H.; Holt, E. A.; Lavin, M.; Morehouse, S. M. *Inorg. Chem.* **1985**, *24*, 1986.
(4) Lee, D.-H.; Chen, J.; Faller, J. W.; Crabtree, R. H. *Chem. Commun.* **2001**, 213.
(5) Cooper, N. J.; Green, M. L. H. *J. Chem. Soc., Chem. Commun.* **1974**, 209.
(6) Cooper, N. J.; Green, M. L. H. *J. Chem. Soc., Chem. Commun.* **1974**, 761.
(7) Cooper, N. J.; Green, M. L. H. *J. Chem. Soc., Dalton Trans.* **1979**, 1121.
(8) Shih, K.-Y.; Totland, K.; Seidel, S. W.; Schrock, R. R. *J. Am. Chem. Soc.* **1994**, *116*, 12103.
(9) Schrock, R. R.; Seidel, S. W.; Mosch-Zanetti, N. C.; Dobbs, D. A.; Shih, K.-Y.; Davis, W. M. *Organometallics* **1997**, *16*, 5195.
(10) Turner, H. W.; Schrock, R. R. *J. Am. Chem. Soc.* **1982**, *104*, 2331.
(11) Turner, H. W.; Schrock, R. R.; Fellman, J. D.; Holmes, S. J. *J. Am. Chem. Soc.* **1983**, *105*, 4942.
(12) Fellman, J. D.; Schrock, R. R.; Traficante, D. D. *Organometallics* **1982**, *1*, 481.

Scheme 1

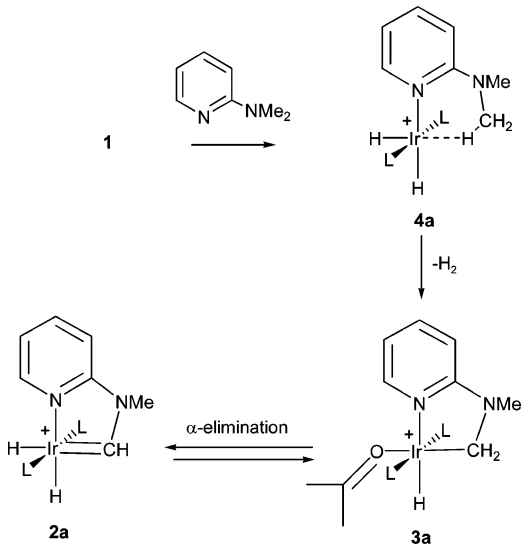

was detected by trapping the alkyl complex with small, two-electron donor ligands. Complex $Cp^*_2(H)Ta{=}C{=}CH_2$/$Cp^*_2Ta{-}CH{=}CH_2$ decomposes via both α-elimination and β-H-elimination, but α-elimination is favored by a factor of 10^8, owing to a highly strained transition state for β-H-elimination.[14] In complexes [{N_3N}Mo(alkyl)] (N_3N^{3-} = [($Me_3SiNCH_2CH_2)_3N]^{3-}$; alkyl = cyclopentyl, cyclohexyl), α-elimination is faster than β-H-elimination; however, no products of α- and β-H-elimination were observed.[15] In some iridium complexes, α-elimination was proposed to be faster than β-H-elimination from D labeling,[16] but later work showed that the results were better explained on the basis of a strongly bound alkane complex as an intermediate.[17] A heteroatom greatly facilitates both CH oxidative addition and α-elimination to give a carbene. Irreversible geminal α-dehydrogenation of several cyclic ethers and amines such as dioxolane, furan, and pyrrolidine by $RuHCl(P^iPr_3)_2$ and $OsH_3Cl(P^iPr_3)_2$ has been observed.[18]

Results

Double Dehydrogenation. A stoichiometric reaction of 2-(dimethylamino)pyridine (py-NMe_2) and $[H_2Ir(OCMe_2)_2(PPh_3)_2]BF_4$ (**1**) yields the cyclic heteroatom-stabilized carbene complex **2a** (Scheme 1). The product is isolated as an air-stable solid in 78% yield after 15 min at 25 °C in CH_2Cl_2. The ^{1}H NMR spectrum of **2a** contains a low field singlet of unit intensity at 11.63 δ assigned to C**H**=Ir and a singlet at 3.39 δ of intensity 3H assigned to the N−Me group. The two inequivalent hydrides resonate at −10.03 δ (trans to C) and −17.85 δ (trans to N) as triplets of doublets ($^2J_{PH}$ = 17.0 Hz, $^2J_{HH'}$ = 4.3 Hz) indicating each hydride is cis to the two phosphines. The ^{13}C NMR spectrum of **2a** exhibits a low-field resonance at 250.5 δ assigned to Ir=C in the characteristic chemical shift range for heteroatom stabilized (Fischer) carbenes. Two resonance forms of **2a** are shown in eq 1: **2″** with an Ir−C single bond, usually dominant in Fischer carbenes, while **2′** has the Ir=C double bond that one would normally expect for a true carbene. Unfortunately, no suitable crystals of **2a** could be grown for crystallographic study.

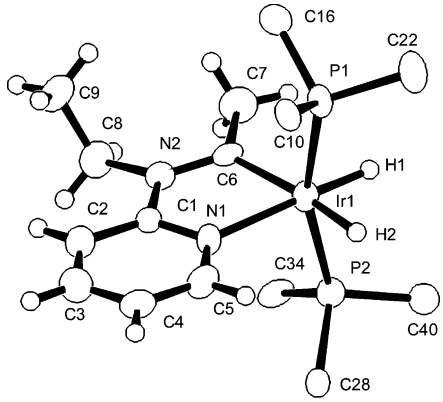

Figure 1. Crystal structure of the cation of the carbene complex **2b**.

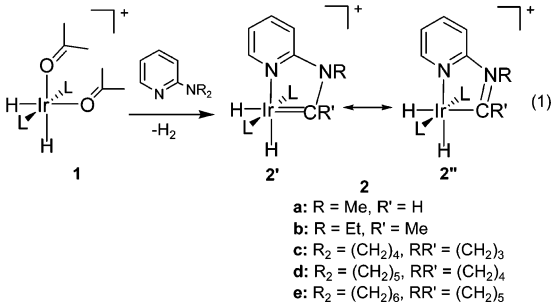

The case of py-NMe_2 gave no opportunity for β-elimination, so we moved to py-NEt_2, where that possibility does now exist. The same reaction proved possible for 2-diethylaminopyridine (py-NEt_2) to give the analogous carbene **2b** at 25 °C after 15 min in CH_2Cl_2 solution in 80% yield (eq 1). The ^{1}H NMR spectrum of **2b** contains two terminal IrH resonances at −10.73 δ (trans to C) and −17.85 δ (trans to N) that are both mutually coupled ($^2J_{HH}$ = 4.5 Hz) and coupled to the cis PPh_3 ligands ($^2J_{PH}$ = 21.4 Hz). The ^{13}C NMR resonance at 265.9 δ is characteristic of a Fischer carbene. Complex **2b** was characterized by an X-ray structure determination (Figure 1). The Ir−C distance of 2.018 Å is consistent with predominant single bond character, while the C−N bond distance of 1.322 Å indicates substantial multiple bond character as expected from the resonance form **2″** generally preferred by Fischer carbenes (eq 1).

The cyclic derivative 2-pyrrolidinopyridine, py-$N(CH_2)_4$, gives the analogous carbene **2c** at 25 °C in 53% yield but only after 7 h (eq 1). The ^{1}H NMR spectrum of **2c** exhibits two high field resonances −9.96 δ (trans to C) and −17.85 δ (trans to N) with coupling constants $^2J_{PH}$ = 20.9 Hz and $^2J_{HH'}$ = 4.7 Hz. The carbene C resonated in the ^{13}C NMR spectrum at 258.3 δ. Complex **2c** was characterized by an X-ray structure determination (Figure 2). The Ir−C distance of 2.151 Å is slightly longer than that in **2b** (2.018 Å), but the C−N bond distances (**2c**, 1.345 Å; **2b**, 1.322 Å) are comparable.

Similarly, cyclic derivatives 2-piperidinopyridine (py-$N(CH_2)_5$) and 2-hexamethyleneiminopyridine (py-$N(CH_2)_6$) form the

(13) van Asselt, A.; Burger, B. J.; Gibson, V. C.; Bercaw, J. E. *J. Am. Chem. Soc.* **1986**, *108*, 5347.
(14) Parkin, G.; Bunel, E.; Burger, B. J.; Trimmer, M. S.; van Asselt, A.; Bercaw, J. E. *J. Mol. Catal.* **1987**, *41*, 21.
(15) Schrock, R. R.; Seidel, S. W.; Mosch-Zanetti, N. C.; Shih, K.-Y.; O'Donoghue, M. B.; Davis, W. M.; Reiff, W. M. *J. Am. Chem. Soc.* **1997**, *119*, 11876.
(16) Burk, M. J.; McGrath, M. P.; Crabtree, R. H. *J. Am. Chem. Soc.* **1988**, *110*, 620.
(17) Gérard, H.; Eisenstein, O.; Lee, D.-H.; Chen, J.; Crabtree, R. H. *New J. Chem.* **2001**, *25*, 1121.
(18) Ferrando-Miguel, G.; Coalter, J. N., III; Gérard, H.; Huffman, J. C.; Eisenstein, O.; Caulton, K. G. *New J. Chem.* **2002**, *26*, 687.

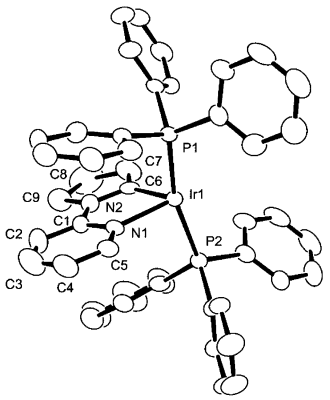

Figure 2. Crystal structure of the cation of the carbene complex **2c**.

Table 1. ^{1}H and ^{13}C NMR Spectroscopic Data for Carbene Complexes[a]

substrate (product)	δ(Ir—H$_t$) (ppm)	δ(Ir—H$_c$) (ppm)	$^2J_{HH}$ (Hz)	$^2J_{PH}$ (Hz)	^{13}C(Ir=C) (ppm)	d(Ir—C) (X-ray, Å)	d(C—N) (X-ray, Å)
Py-NMe$_2$ (**2a**)	−10.03	−17.85	4.3	17.0	250.5		
Py-NEt$_2$ (**2b**)	−10.73	−17.85	4.5	21.4	265.9	2.018	1.322
Py-N(CH$_2$)$_4$ (**2c**)	−9.96	−17.85	4.7	20.9	258.3	2.151	1.345
Py-N(CH$_2$)$_5$ (**2d**)	−10.52	−18.06	4.2	18.4	263.2		
Py-N(CH$_2$)$_6$ (**2e**)	−10.85	−17.89	4.3	18.5	260.4		

[a] H$_t$ is the hydride atom trans to the alkyl carbon, and H$_c$ is the hydride cis to Ir—C

carbene complexes **2d** and **2e**, respectively, at 25 °C after 1 h in the reaction with **1**. Their ^{1}H and ^{13}C NMR data along with those of **2a**−**c** are presented in Table 1.

A cis Intermediate. Computational work described in a separate section predicted that the initial kinetic product of the dehydrogenation reaction should have *cis*-PR$_3$ groups, not trans as at first observed. An effort was therefore made to monitor the reaction to see if any kinetic products could be seen. When the reaction of **1** with py-N(CH$_2$)$_4$ was monitored in situ by ^{1}H NMR spectroscopy, a second isomer, ***cis*-2c**, was indeed identified as the initial kinetic product (eq 2) after 2 h. One hydride in ***cis*-2c** must be trans to a phosphine because it appears as a broad centrosymmetric ^{1}H NMR multiplet (ddd) at −10.83 δ with J_{PH} = 106 Hz (trans P) and 35 Hz (cis P). An irregular intensity pattern, approximately 2:3:3:2, is observed, due to second-order effects caused by the coupled phosphorus nuclei with nearly identical chemical shifts and coupling to protons with different relative signs. The other hydride appears as a triplet of doublets at −18.82 δ with cis coupling constants $J_{PH} \approx J_{P'H}$ = 16 Hz and J_{HH} = 3 Hz. The chemical shift of the latter is typical of H trans to N rather than C as illustrated by a comparison with **2a** for which the values are −10.03 δ, trans to C, and −17.85 δ, trans to N. This is definitely a *cis*-(PR$_3$)$_2$ compound with the stereochemistry shown being the most probable. As the reaction proceeds, the thermodynamic product **2c** grows in at the expense of ***cis*-2c** ($t\{^1/_2\}$ = 3.0 h at 18 °C).

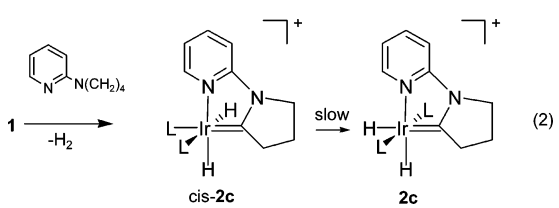

(2)

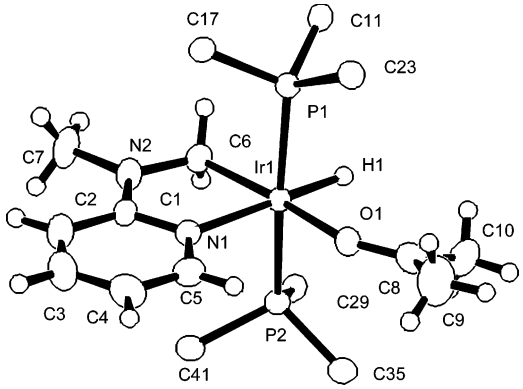

Figure 3. Crystal structure of the cation of the alkyl complex **3a**^{Me_2CO} with acetone as the solvent ligand.

Intermediate Alkyl. The conversion of **1** and py-NMe$_2$ to **2a** was also monitored in situ by ^{1}H NMR spectroscopy, but no *cis*-(PR$_3$)$_2$ products were seen in this case. Free dihydrogen was detected (4.20 δ), consistent with the net loss of H$_2$ on going from **1** to **2a**, in addition to an intermediate alkyl iridium hydride complex [HIr(solv)(py-N(Me)CH$_2$—)L$_2$]BF$_4$ **3a** (solv = Me$_2$CO), denoted **3a**^{Me_2CO}, which disappeared as **2a** was formed. Complex **3a**^{Me_2CO} could be independently prepared in almost quantitative yield by dissolving a pure sample of **2a** in acetone, and in this way, **3a**^{Me_2CO} was isolated and fully characterized (eq 3, L′ = Me$_2$CO). In the ^{1}H NMR spectrum, the terminal hydride of **3a**^{Me_2CO} resonates as a triplet of unit intensity at −16.07 δ, in the range expected for a hydride trans to N, with $^2J_{PH}$ = 15 Hz. No carbene resonance is observed in the ^{13}C NMR spectrum. The molecular structure of **3a**^{Me_2CO} from X-ray diffraction is shown in Figure 3. The d(Ir—C) of 2.072 Å in complex **3a**^{Me_2CO} lies between those of **2b** (2.018 Å) and **2c** (2.151 Å). The d(C—N) of 1.480 Å in **3a**^{Me_2CO} is substantially longer than those in **2b** (1.322 Å) and **2c** (1.345 Å), indicating a single bond character (typical d(C—N) = 1.47 Å).[19]

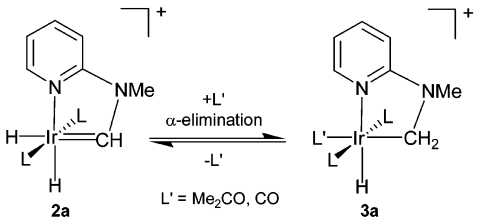

(3)

Agostic Intermediate. The reaction of **1** and py-NMe$_2$ was monitored at low temperature by ^{1}H NMR spectroscopy in an attempt to identify intermediates that occur earlier than **3a**^{Me_2CO}. At −80 °C in CD$_2$Cl$_2$ solution, an agostic species, **4a**, was identified in addition to **3a**^{Me_2CO} (Scheme 1). After 40 min at 0 °C, species **4a** had disappeared, while complexes **3a**^{Me_2CO} and **2a** appeared in the ^{1}H NMR spectrum. Further reaction and warming led to complete conversion to **2a**. Comparison of **4a** with the related structurally characterized authentic agostic complex **4b**,[3] made from 8-methylquinoline via the route shown in Scheme 2, shows close ^{1}H NMR spectral similarities, suggesting **4a** has the agostic (C−H−Ir bridging) structure shown in Scheme 2. For example, the inequivalent hydrides resonate as a pair of signals {**4a**, −20.69 δ (doublet of triplets,

(19) Huheey, J. E.; Keiter, R. L.; Keiter, R. L. *Inorganic Chemistry: Principles of Structure and Reactivity*, 4th ed; Harper Collins College Publishers: New York, 1993.

Scheme 2

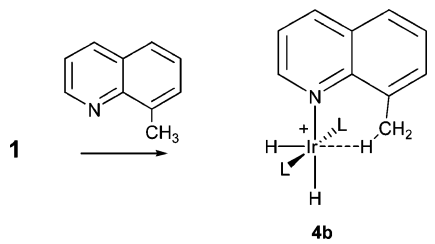

IrH trans to N) and −29.84 δ (doublet of triplets, IrH trans to C−H...Ir) compared with **4b**, −19.20 δ (dt) and −28.60 δ (dt)} coupled both to the two cis phosphines (**4a**, $^2J_{PH}$ = 17.1 Hz; **4b**, $^2J_{PH}$ = 15.0 Hz) and to each other (**4a**, J_{HH} = 7.9 Hz; **4b**, J_{HH} = 8.0 Hz). For **4a** a singlet at 2.60 δ is assigned to the rapidly exchanging py-NMe_2 methyl groups. No broadening of this peak is observed in the ^{1}H NMR spectrum even at −80 °C in CD_2Cl_2, so −NMe_2 group rotation is fast. In contrast to **4a**, **4b**, having no α-N atom, does not cyclometalate or form a carbene. This means that the nitrogen α to the methyl group in **4a** favors both cyclometalation to give the alkyl as well as α-elimination to give the carbene.

Equilibration of 2 and 3. We find an equilibrium between $\mathbf{3a}^{\mathbf{Me_2CO}}$ and **2a** that is highly sensitive to acetone concentration (eq 3, L′ = Me_2CO; Scheme 1). The colorless alkyl complex $\mathbf{3a}^{\mathbf{Me_2CO}}$ dissolved in CD_2Cl_2 loses acetone within seconds to give the yellow carbene **2a**. Addition of 4, 6, and 8 equiv of acetone to a CD_2Cl_2 solution of **2a** yield a $\mathbf{3a}^{\mathbf{Me_2CO}}$/**2a** ratio of 2:1, 3.2:1, and 4.3:1, respectively, qualitatively demonstrating the equilibration. The equilibrium between $\mathbf{3a}^{\mathbf{Me_2CO}}$ and **2a** was also studied more quantitatively using variable temperature ^{31}P NMR spectroscopy in 1,2-dichlorobenzene solution with the result that $\Delta H° = -13.0 \pm 0.2$ kcal mol^{-1} and $\Delta S° = -35.0 \pm 1.0$ cal K^{-1} mol^{-1}. The Gibbs free energy difference between **3a** and **2a** at 298 K is therefore $\Delta G°_{298K} = -3$ kcal mol^{-1}.

We failed to detect any iridium(III) alkyl intermediates in the reaction of **1** with py-NEt_2, py-$N(CH_2)_4$, $N(CH_2)_5$, or $N(CH_2)_6$, in CD_2Cl_2 or from **2b**−**e** in acetone. Using the more basic solvent d_3-acetonitrile, the alkyl hydride *trans*-[(H)Ir(MeCN-d_3)(−CH(CH_3)N(Et)py)(PPh_3)]BF_4 ($\mathbf{3b}^{\mathbf{CD_3CN}}$) was formed from **2b** over 150 min via a retro α-elimination analogous to that of eq 3 with L′ = CD_3CN. The ^{1}H NMR spectrum of $\mathbf{3b}^{\mathbf{CD_3CN}}$ is similar to that of $\mathbf{3a}^{\mathbf{Me_2CO}}$ including a characteristic high field Ir−H resonance (trans to N) at −16.44 δ with coupling constant $^2J_{PH}$ = 15.2 Hz. Attempts to isolate other iridium(III) alkyl complexes from dissolution of **2c** in a variety of donor solvents were unsuccessful, but on the other hand, the alkyl complexes $\mathbf{3d}^{\mathbf{CD_3CN}}$ (from py-$N(CH_2)_5$) and $\mathbf{3e}^{\mathbf{CD_3CN}}$ (from py-$N(CH_2)_6$) were detected from their respective carbenes **2d** and **2e** in d_3-acetonitrile solvent, forming over a time period of ca. 5 h. The reason that reversible α-elimination is not observed with **2c**, having a five-membered ring, but only with the acyclic amines (**2a**−**2b**) and the larger cyclic amines (**2d**−**e**), is probably the ring strain that would occur if the alkyl complex formed from **2c**. This alkyl would have a strained fused 5:5 ring system, while those from **2d**−**e** would have less strained 5:6 or 5:7 ring systems; the acyclic cases, lacking ring fusion, would be even less strained.

The reversibility of the reaction in eq 3 (L′ = Me_2CO) was monitored by in situ ^{1}H and by ^{31}P NMR experiments. Dissolution of yellow crystals of **2a** in d_6-acetone yields a colorless solution of alkyl hydride [HIr($OCMe_2$)(py-N(Me)CH_2−)L_2]BF_4 ($\mathbf{3a}^{\mathbf{(CD_3)_2CO}}$), as confirmed by its ^{31}P NMR resonance at 17.78 δ. After hydrogen was bubbled through this solution for 30 min, the formation sequence was almost completely reversed to give dihydride [IrH_2($OC(CD_3)$)$_2$(PPh_3)$_2$]BF_4 (**1**-d_{12}), alkyl hydride $\mathbf{3a}^{\mathbf{(CD_3)_2CO}}$, and free py-$NMe_2$ in a 1:1:1 ratio, identified from their ^{1}H and ^{31}P NMR spectra. This reversibility of py-NMe_2 binding is of course required for isotope exchange catalysis to occur.

H/D Exchange. Deuterium labeling experiments were carried out to determine the fate of the terminal hydrides of **1** during the reaction with substrates py-NMe_2, py-NEt_2, and py-$N(CH_2)_4$ to generate complexes **2a**−**c**, respectively. Complex [D_2Ir($OCMe_2$)$_2$(PPh_3)$_2$]BF_4 (**1**-d_2), prepared from [Ir(cod)(PPh_3)$_2$]BF_4 and D_2 in acetone, reacted with py-NMe_2 in CH_2Cl_2 solution over 15 min to yield $\mathbf{3a}^{\mathbf{(CD_3)_2CO}}$. The ^{1}H NMR data for the NMe region of $\mathbf{3a}^{\mathbf{(CD_3)_2CO}}$ show that 4% of the NMe sites are deuterated, as confirmed by the appearance of a singlet at 3.46 δ in the ^{2}H NMR spectrum. There were no Ir-D resonances in the high field region of the ^{2}H NMR spectrum. Similar results were obtained from **1**-d_2 and py-NEt_2, where deuterium incorporation occurred to some extent (5%) at the NEt methylene group.

In the case of py-$N(CH_2)_6$, the methylene protons adjacent to the carbene carbon were also slightly deuterated (ca. 5%) appearing as a singlet at 3.59 δ in the ^{2}H NMR spectrum. No deuterium incorporation was observed at the β-carbon position for either the py-NEt_2 or py-$N(CH_2)_4$ cases, demonstrating the selectivity of the deuterium incorporation for complex **1**-d_2.

CO Experiments. During the computational study, it became clear that dissociation of the pyridine arm of the chelate might be of importance. To check this, we passed CO (1 atm) through CH_2Cl_2 solutions of the carbene complexes **2a**−**c**. The carbenes from acyclic py-NMe_2 and py-NEt_2 underwent immediate reaction (seconds) to give [HIr(CO)(py-N(Me)CH_2−)L_2]BF_4, $\mathbf{3a}^{\mathbf{CO}}$, (eq 3, L′ = CO) the CO analogue of the acetone complex, $\mathbf{3a}^{\mathbf{Me_2CO}}$. The cyclic carbene **2c** derived from py-$N(CH_2)_4$ was completely inert even after a 10 h reaction time. The lack of reactivity of the latter implies that either (i) the pyridine is never labile at all or, more probably, (ii) that the pyridine is labile but the bulk of the pyridine, held by the five-membered ring in a conformation that forces the pyridine to point to the metal, cannot freely rotate to become coplanar with the ML_2(carbene) plane as would be required for the α-H transfer to occur (Scheme 3). Models show that the pyridine is far more free to move so as to point away from the metal in the acyclic cases (**2a**−**b**) but is severely restricted in the five-membered cyclic case (**2c**). We therefore propose that pyridine is lost in these acyclic complexes, allowing CO to bind. After carbene rotation, retro α-elimination would lead directly to the observed carbonyl (Scheme 3, L′ = CO).

Confirmation of this picture came from the reaction of CO with the cis carbene, ***cis*-2c**, observed after short reaction times from **1** and py-$N(CH_2)_4$. ***cis*-2c** reacts with CO (1 atm, 10 min) to undergo retro α-elimination to give the previously unobserved alkyl as the CO adduct, $\mathbf{3c}^{\mathbf{CO}}$. In contrast, under the same conditions, the trans carbene, **2c**, is entirely unreactive. This implies that retro α-elimination requires the reacting Ir−H bond to be orthogonal to the carbene plane and aligned with the empty p-orbital of the carbene carbon, as in ***cis*-2c**.

Scheme 3

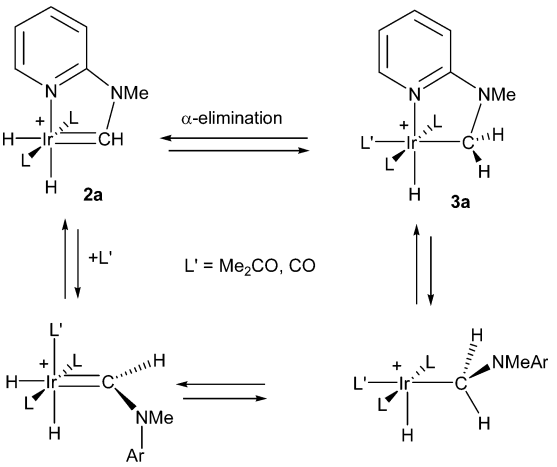

Scheme 4

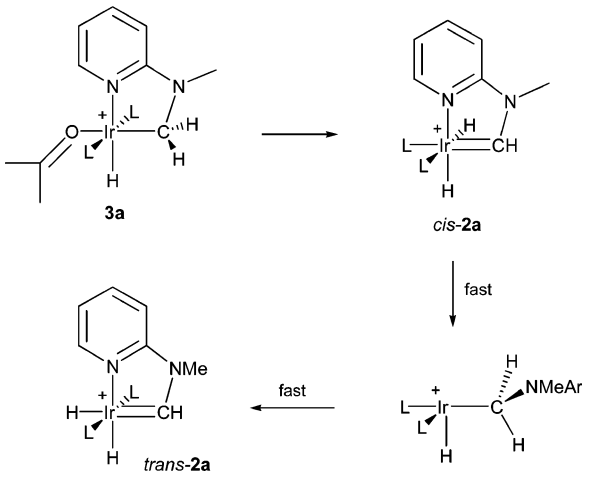

This in turn implies that slow pyridine dissociation is the factor that makes cis to trans isomerization of the product carbene in the reaction of eq 2 slow in the cyclic case, permitting observation of a cis intermediate that only slowly ($t\{^1/_2\} = 3.0$ h at 18 °C) converts to the trans form. In the acyclic case, the same pathway via the cis intermediate may be followed, but the subsequent isomerization to the observed trans compound is now very fast because the pyridine is very labile and rotation around the Ir−C single bond is facile (Scheme 4).

Computational Studies. Unless stated, all the complexes in the DFT study involve PH_3 and py-NMe_2 and are designated with the experimental numbering scheme followed by **t** (**1t**, **2t**,...). The experimental species have been calculated including all atoms at the DFT level. Selected structures have been calculated with PMe_3 and PPh_3 at the DFT level. We give both *E* and *G* values because *G* is indispensable here, owing to the gain or loss of ligands during the overall process.

In complex **1t**, the two cis ketone ligands each have typical Ir−O−C angles of ca. 130°. Replacement of the two ketones by a py-NMe_2 with bound pyridine and agostic C−H, **4t**, destabilizes the system by $\Delta E = 14$ kcal mol^{-1}. However the change in free energy is only $\Delta G = 3.1$ kcal mol^{-1} because of the favorable entropy for decoordination of two acetone molecules. This py-NMe_2 agostic complex, **4t**, the starting point for the mechanistic study, is the energy reference for *E* and *G* ($E = -14.0$ kcal mol^{-1} and $G = -3.1$ kcal mol^{-1} for **1t**). In

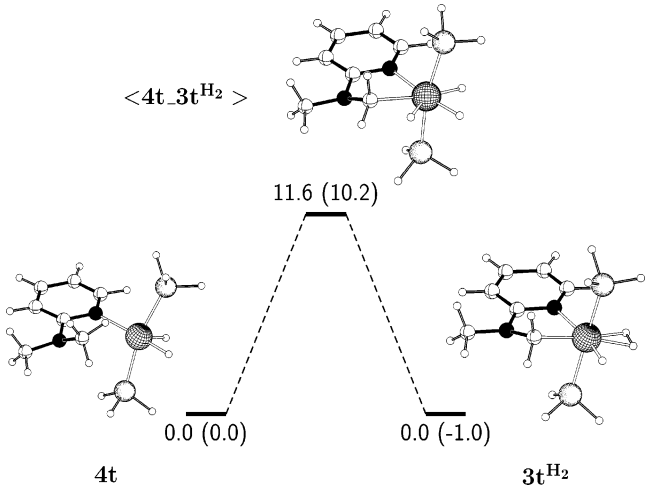

Figure 4. Energy profile (kcal mol^{-1}) for C−H activation from $[H_2Ir(py\text{-}NMe_2)(PH_3)_2]^+$, **4t**. Gibbs free energies are given in parentheses.

complex **4t**, the agostic C−H bond of the py-NMe_2 that is close to the metal has Ir...C = 2.766 Å and Ir...H = 2.013 Å (Figure 4). The C−H bond is twisted out of the Ir−py−N plane to allow the metal to bind side-on to access the C−H bond electronic density and avoid the Ir...H distance being too short. The transition state for cleaving the C−H bond, designated as <**4t_3t**$^{\mathbf{H_2}}$>, has been located at $\Delta E = 11.6$ kcal mol^{-1} ($\Delta G = 10.2$ kcal mol^{-1}) above **4t** and has Ir^V character[20] with the angles between the five ligands in the equatorial plane ranging from 90° to 46°, the latter being C−Ir−H of the C−H bond to be cleaved (Figure 4). The distances between the three hydrogens are longer than 1.8 Å, and the C...H distance of the activated bond is 1.617 Å. The Ir−C (2.246 Å) as well as the Ir−H bonds (1.603 Å) are almost fully formed, with the latter being very close to the two other *d*(Ir−H). This transition state <**4t_3t**$^{\mathbf{H_2}}$> leads to a dihydrogen complex, **3t**$^{\mathbf{H_2}}$, isoenergetic with complex **4t** ($\Delta E = 0.$ kcal mol^{-1}, $\Delta G = -1.0$ kcal mol^{-1}). In **3t**$^{\mathbf{H_2}}$, the dihydrogen is trans to the Ir−C bond and lies in the py−N−C plane (Figure 4). The Ir−C bond is short (2.086 Å) because the trans H_2 ligand has a very weak trans influence. The geometry of the complex is essentially octahedral. H_2 with its weak binding energy ($\Delta E = 17.9$ kcal mol^{-1}, $\Delta G = 5.1$ kcal mol^{-1}) is easily lost, and therefore the acetone lost earlier can readily bind. In agreement with experiment, the acetone complex **3t**$^{\mathbf{Me_2CO}}$ is calculated to be more stable than **3t**$^{\mathbf{H_2}}$ ($\Delta E = -8$ kcal mol^{-1}, $\Delta G = -2.7$ kcal mol^{-1}).

From this point two pathways can be envisaged, one via **3t**$^{\mathbf{H_2}}$ and the other from **3t**$^{\mathbf{Me_2CO}}$. Despite our efforts, no pathway could be identified leading from **3t**$^{\mathbf{Me_2CO}}$ to the carbene complex **2t**. In the first pathway, when H_2 is lost from **3t**$^{\mathbf{H_2}}$, the empty coordination site of the octahedron, represented by an open square □, in the resulting 16-e square pyramid **3t**$^{\square}$, is trans to the alkyl ligand, so no vacant cis site is available for the α-H migration and a geometrical rearrangement is thus needed (Figure 5). The pyridine cannot dissociate because the resulting 14-e species would be very unstable, so the only way to create an empty site cis to the Ir−CH_2 bond is to move one of the phosphine ligands toward the empty site created by the departure of H_2. The appropriate transition state, <**3t**$^{\square}$***_cis*-2t**>, for the resulting C−H cleavage has been located only 3.6 kcal mol^{-1}

(20) Lam, W. H.; Jia, G.; Lin, Z.; Lau, C. P.; Eisenstein, O. *Chem.—Eur. J.* **2003**, *9*, 2775.

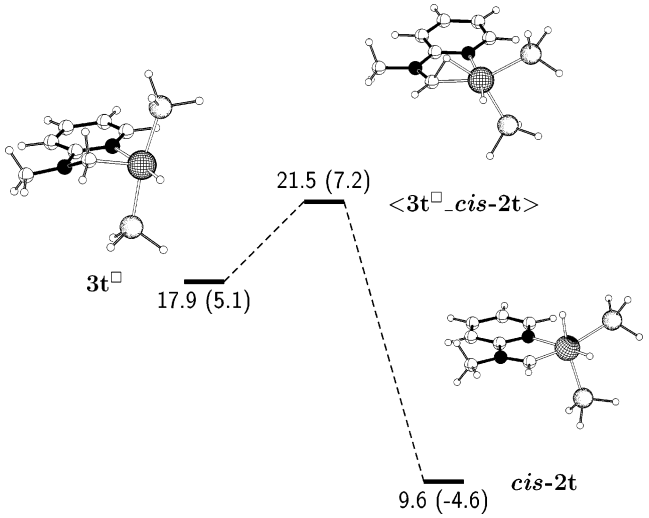

Figure 5. Energy profile (kcal mol^{-1}) for α-C−H migration from [HIr(py-NMe-CH$_2$−)(PH$_3$)$_2$]$^+$, **3t**$^{\square}$**.** Gibbs free energies are given in parentheses.

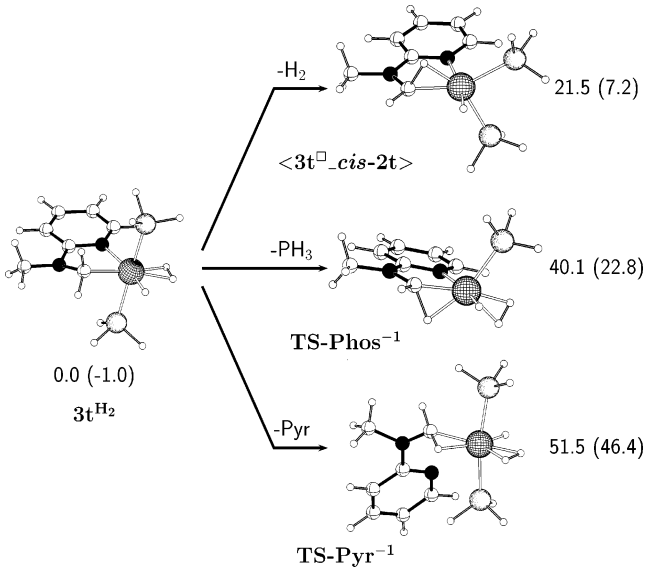

Figure 6. Relative energy (kcal mol^{-1}) of the TS for α-C−H migration associated with loss of a ligand (H_2 (top), PH_3 (middle), or pyridine (bottom)) from [H(H$_2$)Ir(py-NMe-CH$_2$−)(PH$_3$)$_2$]$^+$, **3t**$^{\mathbf{H_2}}$. Gibbs free energies are given in parentheses.

(ΔG = 2.1 kcal mol^{-1}) above the 16-e complex **3t**$^{\square}$ (Figure 5). In this transition structure, the two phosphine ligands are cis (P−Ir−P = 93.6°). In complex **3t**$^{\square}$, the dihedral angles C−N(py)−Ir−P are 107° and 70° indicating that the two phosphines could be considered as being perpendicular to the py−N−Ir plane. In <**3t**$^{\square}$***_cis*-2t**>, these two angles have become 67° and 30°, which shows that both the phosphines move significantly relative to the pyridine plane during the α-H migration. The C−H bond is only moderately elongated (1.347 Å), and the newly forming Ir−H bond is 1.779 Å. The Ir−C bond has shortened from 2.040 Å in **3t**$^{\square}$ to 1.967 Å in <**3t**$^{\square}$***_cis*-2t**>. This transition state connects with a dihydrido−carbene complex ***cis*-2t**, having two cis phosphines. Complex ***cis*-2t** is octahedral with all the high trans influence ligands, carbene and hydride, trans to weak trans influence ligands, phosphine and pyridine, a favorable arrangement. The Ir−C bond length (2.005 Å) is essentially the same as the experimental value of 2.018 Å. The C−N bond has also shortened significantly from **3t**$^{\square}$ (1.452 Å) to ***cis*-2t** (1.338 Å). The C−N bond distance is marginally longer than the experimental value of 1.322 Å. This illustrates the strong donation by N and Ir into the empty carbene orbital. The energy of ***cis*-2t** is calculated to be 8.3 kcal mol^{-1} (ΔG = −9.7 kcal mol^{-1}) below the 16-e complex **3t**$^{\square}$. The cleavage of the C−H bond in the alkyl complex is thus favorable, having a small energy barrier. The complex having two trans phosphine ligands, **2t**, is found 5.4 kcal mol^{-1} (ΔG = 5 kcal mol^{-1}) above ***cis*-2t**.

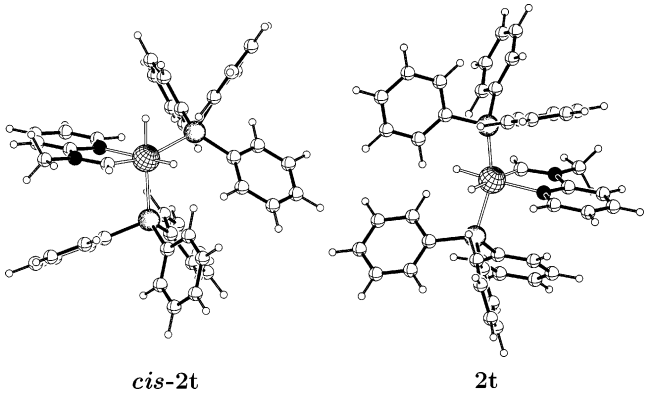

Figure 7. DFT(B3PW91) optimized geometries for [(H)$_2$Ir(py-NMe-CH−)(L)$_2$]$^+$, **2t** and ***cis*-2t**, for L = PPh_3.

Table 2. Selected Full DFT(B3PW91) Optimized Structural Parameters of [H$_2$Ir(pyr-NMe-CH═)L$_2$]$^+$, **2t**, with trans and cis L Ligands[a]

	L = PH_3		L = PMe_3		L = PPh_3	
	trans	cis	trans	cis	trans	cis
Ir−C6	2.004	1.949	1.980	1.941	1.991	1.940
Ir−N1	2.177	2.190	2.172	2.199	2.166	2.208
C6−N2	1.338	1.335	1.350	1.343	1.342	1.336
Ir−H1	1.583	1.582	1.581	1.579	1.576	1.607
Ir−H2	1.655	1.608	1.663	1.615	1.649	1.607
Ir−P1	2.308	2.370	2.336	2.400	2.357	2.431
Ir−P2	2.308	2.382	2.336	2.405	2.341	2.449
P1−Ir−P2	153.9	94.1	153.2	96.7	156.8	104.5
ΔE	0.0	−5.4	0.0	+1.7	0.0	+4.3

[a] Energy differences, ΔE, in kcal mol^{-1}. The numbering scheme is that shown in Figure 1.

Alternate pathways for the C−H cleavage starting from the 18-e alkyl Ir complex, **3t**$^{\mathbf{H_2}}$, could in principle be initiated by loss of either phosphine or pyridine (Figure 6). Transition states associated with the C−H cleavage in these 16-e species with a dissociated phosphine (**TS−Phos**$^{-1}$) or dissociated pyridine (**TS−Pyr**$^{-1}$) have been located 18.6 kcal mol^{-1} (ΔG = 15.6 kcal mol^{-1}) and 30 kcal mol^{-1} (ΔG = 39.2 kcal mol^{-1}) above the transition state <**3t**$^{\square}$***_cis*-2t**>. The high values rule out loss of these ligands and clearly indicate a preferential passage through <**3t**$^{\square}$***_cis*-2t**> for the α-migration of H from the alkyl complex **3t**$^{\mathbf{H_2}}$. The initial dissociation of H_2 is thus favored. Because of the high energies of **TS-Phos**$^{-1}$ and **TS-Pyr**$^{-1}$, no 16-e complexes from the dissociation of the phosphine or the pyridine were optimized.

The relative energies of the cis and trans isomers ***cis*-2t** and **2t** vary with the nature of the phosphine. While the cis isomer is favored by 5.4 kcal mol^{-1} for PH_3, the trans isomer is favored by 1.7 kcal mol^{-1} and 4.3 kcal mol^{-1} for PMe_3 and PPh_3, respectively (see Figure 7 and Table 2). The angle P−Ir−P in the cis complex increases with the size of the phosphine (94.1° for PH_3, 96.7° for PMe_3, 104.5° for PPh_3), supporting an

electronic preference for the cis isomer, overcome by steric effects.[21] The preference for the cis isomer is associated with the optimal relative positioning of strong and weak ligands.

Discussion

The calculations predicted that the *cis*-phosphine isomer is initially formed, a proposal subsequently supported by the experimental evidence for py-N$(CH_2)_4$. However, the cyclic amine, py-N$(CH_2)_4$, is the only one for which the *cis*-phosphine intermediate ***cis*-2t** was observed. Two possibilities exist. Either the other amines go directly to the trans complex or all go via the cis intermediate but the cis to trans isomerization is very fast. The CO experiments only test for the presence of an empty coordination site and so cannot safely distinguish between the two pathways because both require such an empty site.

The first possibility, a direct trans process, cannot be excluded (although despite numerous attempts, no corresponding transition state could be located) because once the pyridine dissociated in $\mathbf{3t^{Me_2CO}}$, the alkyl can rotate so as to allow the α-H migration to occur without phosphines having to move (Scheme 3). If so, py-N$(CH_2)_4$ is unable to follow this direct trans pathway. We propose that the conformational constraints of the cyclic amine py-N$(CH_2)_4$ prevent the dissociated pyridine from rotating away from the metal, a rotation that would be required in order for the carbene to achieve a conformation suitable for the α-H migration with Ir−H aligned with the vacant carbene p-orbital. In this required conformation, the pyridine group would collide with the trans PPh_3 groups. This steric problem which only occurs for the conformationally restrained py-N$(CH_2)_4$ case also explains why CO does not react with **2c**, while the acyclic cases **2a**−**b** give the alkyl complex $\mathbf{3^{CO}}$.

The second possibility, that cis to trans isomerization is fast, should also be considered because a pathway for such a process involving decoordination of the pyridine exists (Scheme 4). In this proposal, the conformationally mobile cases (**2a**−**b**, **2e**−**d**) give fast rearrangement, but the **2c** case (py-N$(CH_2)_4$) is slow because of steric hindrance of Ir−C bond rotation by the dissociated pyridine. An alternative pathway for cis to trans isomerization, with rate-determining loss of PPh_3, can be excluded because this pathway should not show a large rate difference between ***cis*-2c** and ***cis*-2a**−**b**. In addition, the observed rate of isomerization is unaffected by the addition of PPh_3 (5 equiv).

As expected, the free energy *G*, which includes the entropy changes associated with the gain or loss of ligands during the reaction, should be considered in preference to the energy *E*. The calculations show that the difference in free energy between the most stable product $\mathbf{3t^{Me_2CO}}$ and the highest transition state $<\mathbf{3t^{\square}\_cis\text{-}2t}>$ is only 10.9 kcal mol^{-1}, while the difference in energy *E* is 29.5 kcal mol^{-1}. This is consistent with the reversibility of the reactions, implied by the catalysis and directly observed for species $\mathbf{3^{Me_2CO}}$ and **2**.

The energies of **4** and **3** are the same because the C−H and H−H as well as Ir−C and Ir−H bond energies are similar and because the Ir−N−C−N−C five-membered ring is unstrained. The transition state is relatively low due to the accessibility of Ir^V for iridium with strongly σ-donating ligands, such as in the very stable IrH_5L_2.[22] The overall transformation of **4** to **3** can thus be viewed as H transfer from an alkyl group to a hydride ligand. The calculations indicate that an oxidative addition/reductive elimination is preferred over the alternative σ-metathesis process. The formation of a dihydrogen complex and the loss of H_2 during the reaction path are supported experimentally by the observation of H_2. Another rationalization of the equivalent energies of **4** and **3** is the optimal distribution of strong and weak trans influence ligands around the metal.[23] In **4**, the weak trans influence agostic ligand is trans to a high trans influence hydride. In **3**, the agostic ligand converts to a high trans influence alkyl group, but trans to this alkyl is now the H_2 group with the smallest trans influence of all ligands. In this transformation, the high and low trans influence ligands just trade places via H migration.

The energies of the alkyl and the carbene complexes are similar because the N lone pair stabilizes the carbene group. In related geminal dehydrogenations of furan and pyrrolidine by $[RuHCl(P^iPr_3)_2]_2$ and $OsH_3Cl(P^iPr_3)$, calculations have shown why the reaction is feasible.[18]

The reversibility of the reaction is also supported by the H/D scrambling and the tritiation catalysis whereby D(T) originally on the metal is transferred to the Me group of the amine. The H/D scrambling is made possible by the very facile H/H′ exchange in species such as **3**. This includes a rotation of the H_2 ligand and H/H′ exchange between the hydride and H_2. We did not study this computationally in this species, but there are ample examples in similar complexes.[24]

The cis and trans $(PR_3)_2$ are close in energy because of the bulk of the phosphine ligand. The cis isomer has the best distribution of strong and weak trans influence ligands in the coordination sphere of Ir and is favored electronically; the trans isomer becomes favored solely on steric grounds. This explains why the difference in energy between these two isomers is not very large even for PPh_3. Apart from illustrating the limitations and advantages of using PH_3 as model phosphine, this work suggests that it may sometimes be necessary to search for kinetic isomers with cis phosphines in mechanistic studies even if both reagents and products have trans phosphines. This may occur if the isomerization produces a favorable distribution of strong and weak trans influence ligands.

Experimental Section

All preparations and manipulations were carried out under oxygen-free nitrogen or argon following conventional Schlenk techniques. Dichloromethane was freshly distilled from CaH_2 and degassed before use. Diethyl ether was dried over sodium and benzophenone and degassed before use. Deionized water was used. 2-(Dimethylamino)-pyridine, 2-chloropyridine, and pyrrolidine were purchased from Aldrich. 2-Diethylaminopyridine was obtained from ITC Corp. Cyclic pyridines (py-N$(CH_2)_n$)[25] and the complexes $[IrH_2(OCMe_2)_2L_2]BF_4$ (**1**)[26] and $[Ir(COD)L_2]BF_4$ (**2**) (L = PPh_3)[27] were prepared according to literature procedures. ^{1}H NMR, ^{13}C{^{1}H} NMR,^{31}P{^{1}H} NMR, and

(21) QM/MM calculations of the cis versus trans **2a** (L = PPh_3) predict a preference for the cis form in disagreement both with experiment and with the full DFT calculations. The origins of this discrepancy are under study.

(22) Garlaschelli, L.; Khan, S. I.; Bau, R.; Longoni, G.; Koetzle, T. F. *J. Am. Chem. Soc.* **1985**, *107*, 7212.
(23) Matthes, J.; Gründemann, S.; Toner, A.; Guari, Y.; Donnadieu, B.; Spandl, J.; Sabo-Etienne, S.; Clot, E.; Limbach, H.-H.; Chaudret, B. *Organometallics* **2004**, *23*, 1424.
(24) Maseras, F.; Lledós, A.; Clot, E.; Eisenstein, O. *Chem. Rev.* **2000**, *100*, 601.
(25) Hassner, A.; Krepski, L. R.; Alexanian, V. *Tetrahedron* **1978**, *34*, 978.
(26) Crabtree, R. H.; Demou, P. C.; Eden, D.; Mihelcic, J. M.; Parnell, C. A.; Quirk, J. M.; Morris, G. E. *J. Am. Chem. Soc.* **1982**, *104*, 6994.
(27) Crabtree, R. H. *Synth. React. Inorg. Met. -Org. Chem.* **1982**, *12*, 407.

heteronuclear two-dimensional NMR were recorded on Bruker 400, Bruker 500, GE-Omega 300, or GE-Omega 500 spectrometers. Microanalyses were carried out by Robertson Microlit Laboratories.

***cis,trans*-[Dihydridobis(triphenylphosphine)(*N,C*-2-(dimethylamino)pyridine-1′-ylidene)iridium(III)] Fluoroborate (2a).** Method 1: The fluoroborate salt of $[H_2Ir(OCMe_2)_2(PPh_3)_2]^+$ (**1**) (280 mg, 0.30 mmol) was dissolved in degassed CH_2Cl_2 (4 mL), and 2-(dimethylamino)pyridine (py-NMe_2, 37 mg, 0.30 mmol) was added. The resulting clear yellow solution was stirred for 15 min. Slow addition of diethyl ether (ca. 10 mL) gave a light yellow precipitate. The solution was then filtered, and the light yellow powder was washed with Et_2O (15 mL) and dried in vacuo to give pure product. The complex was recrystallized from CH_2Cl_2/Et_2O. Yield: 217 mg (78%).

Method 2: to a clear red CH_2Cl_2 (10 mL) solution of $[Ir(COD)(PPh_3)_2]BF_4$ (**2**) (352 mg, 0.38 mmol) was syringed py-NMe_2 (50 mg, 0.38 mmol). H_2 gas was passed for 10 min at 0 °C, and the solution turned bright yellow. After warming to room temperature, diethyl ether (10 mL) was added to give a yellow solid, which was filtered, washed with diethyl ether (3 × 8 mL), and dried in vacuo. Yield: 140 mg (40%).

^{1}H NMR (CD_2Cl_2) δ 11.63 (s, 1H, ═C*H*), 7.65 (t, 1H, J_{H-H} = 7.9 Hz, pyridine─*H*), 7.50 (d, 1H, J_{H-H} = 6.1 Hz, pyridine─*H*), 7.28 (m, 31H, P*Ph*$_3$ and pyridine─*H*), 6.48 (t, 1H, J_{H-H} = 6.7 Hz, pyridine─*H*), 3.39 (s, 1H, Ir═C(H)N(*Me*)py), −10.03 (td, 1H, J_{P-H} = 17.0 Hz, J_{H-H} = 4.3 Hz, Ir─*H* (trans to Ir═CH)), −17.85 (td, 1H, J_{P-H} = 17.0 Hz, J_{H-H} = 4.3 Hz, Ir─*H* (trans to Ir─N)); ^{13}C{^{1}H} NMR (CD_2Cl_2) δ 250.46 (s, Ir═*C*), 154.82 (s, C_{py}2), 154.41 (s, C_{py}6), 137.99 (s, C_{py}5), 132.62 (s, C_{Ph}1), 132.28 (t, J_{P-C} = 6.0 Hz, C_{Ph}2,6), 129.80 (s, C_{Ph}4), 127.60 (t, J_{P-C} = 6.0 Hz C_{Ph}3,5), 123.23 (s, C_{py}4), 113.22 (s, C_{py}3), 46.46 (s, Ir═C(H)N(*Me*)py). ^{31}P{^{1}H} NMR (CD_2Cl_2) δ 21.80. Anal. Calcd for $C_{43}H_{40}N_2P_2IrBF_4 \cdot O_1C_4H_{10}$: C, 56.46; H, 5.00; N, 2.80. Found: C, 56.62; H, 4.68; N, 2.91.

***cis,trans*-[Dihydridobis(triphenylphosphine)(*N,C*-2-diethylaminopyridine-1′-ylidene)iridium(III)] Fluoroborate (2b).** To $[H_2Ir(OCMe_2)_2(PPh_3)_2]BF_4$ (**1**) (350 mg, 0.38 mmol) dissolved in 5 mL of CH_2Cl_2 2-diethylaminopyridine (py-NEt_2, 60 mg, 0.38 mmol) was added. After 15 min of stirring at room temperature, 10 mL of diethyl ether was added dropwise to give a bright yellow solid. The solution was then filtered leaving a yellow solid, which was washed with diethyl ether (3 × 5 mL) followed by drying in vacuo. The complex was recrystallized from CH_2Cl_2/Et_2O. Yield: 290 mg (80%).

2b can also be prepared by Method 2 from **1** (100 mg, 0.11 mmol) and py-NEt_2 (17 mg, 0.11 mmol) in 10 mL of CH_2Cl_2. **2b** was isolated upon addition of 50 mL of diethyl ether after 10 min of H_2 treatment at 0 °C and recrystalized from CH_2Cl_2/Et_2O. Yield: 48 mg (46%).

^{1}H NMR (CD_2Cl_2) δ 7.78 (t, 1H, J_{H-H} = 7.9 Hz, pyridine─*H*), 7.71 (d, 1H, J_{H-H} = 4.9 Hz, pyridine─*H*), 7.37 (m, 31H, P*Ph*$_3$ and pyridine─*H*), 6.53 (t, 1H, J_{H-H} = 6.1 Hz, pyridine─*H*), 3.72 (q, J_{H-H} = 7.3 Hz, 2H, Ir═C(Me)N(C*H*$_2$CH$_3$)py), 2.24 (s, 3H, Ir═C(*Me*)N(CH$_2$CH$_3$)py), 1.11 (t, J_{H-H} = 7.3 Hz, 3H, Ir═C(Me)N(CH$_2$C*H*$_3$)py), −10.73 (td, 1H, J_{P-H} = 21.4 Hz, J_{H-H} = 4.5 Hz, Ir─*H* (trans to Ir═C)), −17.85 (td, 1H, J_{P-H} = 21.4 Hz, J_{H-H} = 4.5 Hz, Ir─*H* (trans to Ir─N)); ^{13}C{^{1}H} NMR (CD_2Cl_2) δ 265.88 (s, Ir═*C*), 158.48 (s, C_{py}2), 155.77 (s, C_{py}6), 139.78 (s, C_{py}5), 133.84 (t, J_{P-C} = 6.0 Hz, C_{Ph}2,6), 133.60 (s, C_{Ph}1), 131.27 (s, C_{Ph}4), 129.08 (t, J_{P-C} = 6.0 Hz, C_{Ph}3,5), 123.85(s, C_{py}4), 115.18 (s, C_{py}3), 44.66 (s, Ir═C(Me)N(*C*H$_2$CH$_3$)py), 37.95 (s, Ir═C(*Me*)N(CH$_2$CH$_3$)py), 13.22 (s, Ir═C(Me)N(CH$_2$*C*H$_3$)py); ^{31}P{^{1}H} NMR (CD_2Cl_2) δ 20.85. Anal. Calcd for $C_{45}H_{44}N_2P_2IrBF_4$: C, 56.61; H, 4.61; N, 2.94. Found: C, 56.06; H, 4.61; N, 2.85.

***cis,trans*-[Dihydridobis(triphenylphosphine)(*N,C*-2-pyrrolidinopyridine-1′-ylidene)iridium(III)] Fluoroborate (2c).** $[H_2Ir(OCMe_2)_2(PPh_3)_2]BF_4$ (**1**) (200 mg, 0.22 mmol) and py-$N(CH_2)_4$ (32 mg, 0.22 mmol) were stirred in CH_2Cl_2 (10 mL) at room temperature for 7 h. The solvent was then removed in vacuo. The yellow residue was redissolved in 10 mL of CH_2Cl_2. Et_2O (25 mL) was added dropwise to give a very pale yellow precipitate, which was washed with Et_2O (3 × 5 mL) followed by drying in vacuo. The complex was recrystallized from CH_2Cl_2/Et_2O. Yield: 110 mg (53%).

^{1}H NMR (CD_2Cl_2) δ 7.83 (d, 1H, J_{H-H} = 5.3 Hz, pyridine─*H*), 7.82 (t, 1H, J_{H-H} = 8.0 Hz, pyridine─*H*), 7.37 (m, 30H, P*Ph*$_3$), 7.17 (d, 1H, J_{H-H} = 7.5 Hz, pyridine─*H*), 7.61 (t, 1H, J_{H-H} = 6.4 Hz, pyridine─*H*), 3.64 (t, J_{H-H} = 8.0 Hz, 2H, Ir(═CC*H*$_2$CH$_2$CH$_2$)), 2.43 (t, J_{H-H} = 7.5 Hz, 2H, Ir(═CCH$_2$C*H*$_2$CH$_2$)), 1.64 (t, J = 8.0 Hz, 2H, Ir(═CCH$_2$CH$_2$C*H*$_2$)), −9.96 (td, 1H, J_{P-H} = 20.9 Hz, J_{H-H} = 4.7 Hz, Ir─*H* (trans to Ir═C)), −17.85 (td, 1H, J_{P-H} = 20.9 Hz, J_{H-H} = 4.7 Hz, Ir─*H* (trans to Ir─N)); ^{13}C{^{1}H} NMR (CD_2Cl_2) δ 258.34 (s, Ir═*C*), 155.13 (s, C_{py}6), 154.76 (s, C_{py}2), 139.78 (s, C_{py}5), 133.36 (t, J_{P-C} = 6.0 Hz, C_{Ph}3,5), 133.08 (s, C_{Ph}1), 130.86 (s, C_{Ph}4), 128.66 (t, J_{P-C} = 6.0 Hz, C_{Ph}3,5), 123.26 (s, C_{py}4), 114.50 (s, C_{py}3), 54.62 (s, Ir═C(*C*H$_2$-CH$_2$CH$_2$)Npy), 49.45 (s, Ir═C(CH$_2$*C*H$_2$CH$_2$)Npy), 21.94 (s, Ir═C(CH$_2$-CH$_2$*C*H$_2$)Npy). ^{31}P{^{1}H} NMR (CD_2Cl_2): δ 20.06. Anal. Calcd for $C_{45}H_{42}N_2P_2IrBF_4$: C, 56.73; H, 4.41; N, 2.94. Found: C, 56.46; H, 4.40; N, 2.83.

***cis,trans*-[Dihydridobis(triphenylphosphine)(*N,C*-2-piperidinopyridine-1′-ylidene)iridium(III)] Fluoroborate (2d).** $[H_2Ir(OCMe_2)_2(PPh_3)_2]PF_6$ (440 mg, 0.45 mmol) was dissolved in degassed CH_2Cl_2 (4 mL), and 2-piperidinopyridine (py-$N(CH_2)_5$, 73 mg, 0.45 mmol) was added. The resulting clear yellow solution was stirred for 60 min. Slow addition of hexanes (ca. 20 mL) gave a light yellow precipitate. The solution was then filtered, and the light yellow powder was washed with hexanes 3 times (3 × 15 mL) and dried in vacuo to give pure product. The complex was also recrystallized from CH_2Cl_2/hexane. Yield: 400 mg (90%).

^{1}H NMR (CD_2Cl_2, 400 MHz) δ 7.93 (m, 1H), 7.80 (t, 1H, J = 8 Hz), 7.36 (m, 31H), 6.67 (t, 1H, J = 8 Hz), 3.41 (t, 2H, J = 6 Hz, NC***H***2), 2.67 (m, 2H, ═CC***H***2), 1.45, 0.83 (m, 2H each, NCH_2 (C***H***$_2$)$_2$), −10.52 (td, 1H, J_{P-H} = 20 Hz, $J_{H-H'}$ = 4 Hz, Ir─H), −18.06 (td, 1H, J_{P-H} = 16 Hz, $J_{H-H'}$ = 4 Hz, Ir─H); ^{13}C{^{1}H} NMR (CD_2Cl_2, 100 MHz) δ 262.2 (s, Ir═C), 159.1 (s, C_{py}), 154.6 (s, C_{py}), 139.3 (s, C_{py}), 133.2 (t, J_{P-C} = 6.4 Hz, C_{Ph}2,6), 132.8 (s, C_{Ph}1), 130.7 (s, C_{Ph}4), 128.6 (t, J_{P-C} = 6.4 Hz, C_{Ph}3,5), 123.3 (s, C_{py}), 113.7 (s, C_{py}), 49.5 (s, N***C***H$_2$), 48.1 (s, ═C***C***H$_2$), 21.1, 18.4 (s, NCH$_2$(***C***H$_2$)$_2$); ^{31}P{^{1}H} NMR (CD_2Cl_2) δ 20.95. Anal. Calcd for $C_{46}H_{44}N_2P_3IrF_6$: C, 53.96; H, 4.33; N, 2.74. Found: C, 54.13; H, 4.30; N, 2.79.

***cis,trans*-[Dihydridobis(triphenylphosphine)(*N,C*-2-hexamethyleneiminopyridine-1′-ylidene)iridium(III)] Fluoroborate (2e).** $[H_2Ir(OCMe_2)_2(PPh_3)_2]BF_4$ (150 mg, 0.16 mmol) was dissolved in degassed CH_2Cl_2 (6 mL), and 2-hexamethyleneiminopyridine (py-$N(CH_2)_6$, 28 mg, 0.16 mmol) was added. The resulting clear yellow solution was stirred for 60 min. Slow addition of hexane (ca. 20 mL) gave a light yellow precipitate. The solution was then filtered, and the light yellow powder was washed with hexane 3 times (3 × 10 mL) and dried in vacuo to give pure product. The complex was recrystallized from CH_2Cl_2/hexane. Yield: 127 mg (80%).

^{1}H NMR (CD_2Cl_2, 400 MHz) δ 7.64 (m, 2H), 7.27 (m, 31H), 6.36 (t, 1H, J = 8 Hz), 3.63 (m, 2H, NC***H***$_2$), 2.91 (m, 2H, ═CC***H***$_2$), 1.43, 1.31, 0.46 (m, 2H each, NCH_2 (C***H***$_2$)$_3$), −10.84 (td, 1H, J_{P-H} = 20 Hz, $J_{H-H'}$ = 4 Hz, Ir─H), −17.89 (td, 1H, J_{P-H} = 16 Hz, $J_{H-H'}$ = 4 Hz, Ir─H); ^{13}C{^{1}H} NMR (CD_2Cl_2, 100 MHz) δ 270.7 (s, Ir═C), 158.8 (s, C_{py}), 155.4 (s, C_{py}), 139.2 (s, C_{py}), 134.3 (s, C_{Ph}1), 133.4 (t, J_{P-C} = 6.2 Hz, C_{Ph}2,6), 130.8 (s, C_{Ph}4), 128.7 (t, J_{P-C} = 6.4 Hz, C_{Ph}3,5), 123.2 (s, C_{py}), 114.5 (s, C_{py}), 51.1 (s, ═C***C***H$_2$), 50.9 (s, N***C***H$_2$), 28.9, 24.8, 20.4 (s, NCH$_2$(***C***H$_2$)$_3$); ^{31}P{^{1}H} NMR (CD_2Cl_2) δ 21.3. Anal. Calcd for $C_{47}H_{46}N_2P_2IrBF_4$: C, 57.61; H, 4.73; N, 2.86. Found: C, 57.54; H, 4.50; N, 2.49.

Observation of the Initial Kinetic Product, *cis*-2c, from the Reaction of 2-Pyrrolidinopyridine with $[H_2Ir(OCMe_2)_2(PPh_3)_2]BF_4$ (1). ^{1}H NMR spectroscopy showed that 2-pyrrolidinopyridine (1 equiv) reacted with $[IrH_2(OCMe)_2(PPh_3)_2]BF_4$ in CD_2Cl_2 at 25 °C to give an initial *cis*-PPh_3 isomer that slowly isomerizes to the trans isomer at room temperature over 5 h. The ^{1}H NMR spectrum of the two isomers shows two distinct pairs of high field iridium hydride resonances. One

pair, due to the trans isomer, appear as two triplets of doublets at δ −9.98 and δ −18.57 ($^2J_{P-H}$ = 20.9 Hz, $^2J_{H-H'}$ = 4.7 Hz), each coupled to two trans phosphine nuclei. The other pair, due to the cis isomer, is coupled to two cis phosphine nuclei. In particular, one appears as a broad centrosymmetric multiplet centered at δ −10.83 as a result of being coupled to one trans and one cis phosphorus nucleus. Second-order effects due to two coupled phosphorus nuclei with nearly identical chemical shifts and coupling to protons with different relative signs give rise to an irregular intensity pattern (2:3:3:2). The second hydride appears as a triplet of doublets at δ −18.82, as a result of being coupled to two inequivalent cis phosphine nuclei and the other hydride ($^2J_{P-H} \approx {}^2J_{P'-H}$ = 16 Hz, $^2J_{H'-H}$ = 3 Hz).

***trans*-[Hydrido(acetone)bis(triphenylphosphine)(*N,C*-2-(dimethylamino)pyridine-1′-yl)iridium(III)] Fluoroborate ($3a^{Me_2CO}$).** Method 1: to a red acetone (10 mL) solution of $[Ir(cod)(PPh_3)_2]BF_4$ (346 mg, 0.38 mmol) py-NMe_2 (50 mg, 0.38 mmol) was added via a syringe. Upon passing H_2 gas for 10 min at 0 °C, the solution turned to very pale yellow. Diethyl ether (15 mL) was added, and a white precipitate formed. After filtration, the resulting white solid was washed with diethyl ether (3 × 10 mL) and dried in vacuo. The complex was recrystallized from CH_2Cl_2/Et_2O. Yield: 244 mg (65%).

Method 2: To an acetone (5 mL) solution $[H_2Ir(OCMe_2)_2(PPh_3)_2]BF_4$ (**1**) (120 mg, 0.13 mmol) py-NMe_2 (16 mg, 0.13 mmol) was added. After 15 min of stirring, the resulting colorless solution was precipitated by treatment with Et_2O (20 mL). The white precipitate was collected on a glass frit, washed with Et_2O (3 × 5 mL) and dried in vacuo. Yield: 48 mg (37%).

^{1}H NMR ($OCMe_2$-d_6) δ 8.52 (d, 1H, pyridine—*H*), 7.46 (m, 30H, P*Ph*$_3$), 7.17 (t, 1H, J_{H-H} = 8.0 Hz, pyridine—*H*), 6.48 (t, 1H, J_{H-H} = 5.9 Hz, pyridine—*H*), 5.54 (d, 1H, J_{H-H} = 8.5 Hz, pyridine—*H*), 4.06 (t, 2H, J_{H-H} = 12.3 Hz, Ir—C(*H*$_2$)N(Me)py), 2.17 (s, 3H, Ir—C(H$_2$)N(*Me*)py), 2.09 (s, 6H, Ir—$OCMe_2$), −16.07 (t, 1H, J_{P-H} = 15 Hz, 1H, Ir—*H*); ^{13}C{^{1}H} NMR ($OCMe_2$-d_6) δ 161.05 (s, C_{py}2), 146.18 (s, C_{py}6), 138.05 (s, C_{py}5), 135.16 (t, J_{P-C} = 5.3 Hz, C_{Ph}2,6), 131.86 (s, C_{Ph}4), 130.59 (s, C_{Ph}1), 129.75 (t, J_{P-C} = 4.5 Hz, C_{Ph}3,5), 37.21 (s, Ir—C(H$_2$)N(*Me*)py), 30.38 (s, Ir—$OCMe_2$), 15.99 (s, Ir—C(*H*$_2$)N(Me)py); ^{31}P{^{1}H} NMR ($OCMe_2$-d_6) δ 17.78. Anal. Calcd for $C_{46}H_{48}N_2P_2OIrBF_4$: C, 55.99; H, 4.87; N, 2.84. Found: C, 55.78; H, 4,71; N, 2.85.

Reaction of *cis,trans*-$[H_2Ir(=C(Me)N(Et)py)(PPh_3)_2]BF_4$ (2b) with MeCN-d_3. 2b (20 mg, 0.02 mmol) was dissolved in 0.6 mL of MeCN-d_3 in an NMR tube. The sample, monitored periodically by ^{1}H NMR, showed quantitative formation of *trans*-[(H)Ir(MeCN-d_3)(C(HCH$_3$)N(Et)py)$(PPh_3)_2$]BF_4 ($\mathbf{3b^{CD_3CN}}$) after 150 min. ^{1}H NMR (MeCN-d_3) δ 4.12 (m, 1H, Ir—C*H*Me), 1.80 (q, 2H, J_{H-H} = 7.3 Hz, NC*H*$_2$CH$_3$), 1.09 (d, 3H, J_{H-H} = 7.3 Hz, Ir—CH*Me*), 0.42 (t, 3H, J_{H-H} = 7.3 Hz, NCH$_2$C*H*$_3$), −16.44 (1H, J_{P-H} = 15.2 Hz, Ir—H). A pure solid could not be obtained.

Reaction of 2a with H_2 in Me_2CO-d_6. In an NMR tube, 20 mg (0.02 mmol) of **2a** was dissolved in 0.6 mL of Me_2CO-d_6. The yellow solution turned colorless. ^{1}H NMR spectrum taken after 60 s showed quantitative formation of $\mathbf{3a^{(CD_3)_2CO}}$. A stream of H_2 was then bubbled through the solution for 30 min at room temperature. ^{1}H and ^{31}P NMR measurements showed complete consumption of **2a** with >90% conversion to equimolar **1**, $\mathbf{3a^{(CD_3)_2CO}}$, and free py-NMe_2.

H/D Exchange. py-NMe_2 (28 mg, 0.30 mmol) and d^2-**1** were dissolved in 0.6 mL of degassed CH_2Cl_2 in an NMR tube. ^{2}H NMR measurements after 15 min at room temperature showed no resonance for Ir-D but a singlet at 3.46 δ indicating that the methyl region of NMe was deuterated. There was also a singlet for **2a** at 21 δ in the ^{31}P NMR spectrum. Exhaustive vacuum removal of the volatiles, followed by ^{1}H NMR assay in CD_2Cl_2, showed no starting material but only **1** and >95% conversion to **2a**.

A similar procedure was followed for both py-NEt_2 and py-$(CH_2)_4$. In all cases, both ^{1}H and ^{31}P NMR measurements taken at the completion of the reaction showed >95% formation of the Ir(III) carbene complex, **2b** (for py-NEt_2) or **2c** (for py-$(CH_2)_4$).

^{1}H NMR Study of the Equilibrium of 2a and $3a^{Me_2CO}$. The ^{31}P NMR measurements were taken using a GE-Omega 500 spectrometer at 202 MHz. Solutions for the thermodynamic study were prepared by dissolving **2a** in 1,2-dichlorobenzene and adding appropriate amounts of Me_2CO (0.27 M stock solution in 1,2-dichlorobenzene) and perfluorotriphenylphosphine as the internal standard. The analyses of the equilibrium constants using the required equations were carried out with a nonlinear least-squares fit. The reported errors correspond to 1 standard deviation.

Reaction of 2a−c with CO. 2a−b (0.30 mmol) was dissolved in CD_2Cl_2 (0.3 mL) and a reference ^{1}H NMR spectrum was taken prior to bubbling with CO for 30 s. **2a−b** showed immediate and quantitative conversion to compound $\mathbf{3a-b^{CO}}$. Unlike **2a−b**, compound **2c** showed no change on bubbling with CO even after 19 h. $\mathbf{3a^{CO}}$ was prepared in a pure state as follows: **2a** (28 mg, 0.030 mmol) was dissolved in dichloromethane (8 mL), and CO bubbled for 1 min. Approximately half the solvent was evaporated with a stream of air and the product, $\mathbf{3a^{CO}}$ (25 mg, 0.026 mmol), was recrystallized from dichloromethane/ether, forming translucent white, needlelike crystals. Yield: 87% ^{1}H NMR (CD_2Cl_2, 298 K): δ 7.54 (d, 1H, $^3J_{HH}$ = 6.1 Hz, H_{py}), 7.51−7.36 (m, 31H, H_{ar}, H_{py}), 7.08 (m, 1H, H_{py}), 6.11 (m, 1H, H_{py}), 3.51 (t, 2H, $^3J_{PH}$ = 14.1 Hz, IrCH_2N), 2.01 (s, 3H, NCH_3), −15.08 (t, 1H, $^2J_{PH}$ = 12.7 Hz, IrH); ^{31}P NMR (CD_2Cl_2, 298 K) δ10.32; FTIR (CD_2Cl_2) ν(CO) 2034 cm^{-1}.

To observe the reaction of ***cis*-2c** with CO, $[H_2Ir(OCMe_2)_2(PPh_3)_2]BF_4$ (100 mg, 1 equiv) was dissolved in dichloromethane (16 mL). 2-Pyrrolidinopyridine (1 equiv) in dichloromethane (4 mL) was immediately added. The mixture was stirred for 10 min, and then CO (1 atm) was bubbled (50 mL/min) for 60 min. The resulting compound $\mathbf{3c^{CO}}$ was recrystallized from dichloromethane/diethyl ether to give long white needles. By analogy with the spectroscopic data for $\mathbf{3a^{CO}}$ (NMR fully assigned by 2D experiments), the product was identified as $\mathbf{3c^{CO}}$**.** ^{1}H NMR (CD_2Cl_2, 298 K) δ 7.6−7.34 (m, 31H, aromatic), 7.22 (ddd, 1H, ^3J = 8.7, 7.1 Hz, ^4J = 1.6 Hz, py-H4), 6.22 (ddd, 1H, $^3J_{H-H}$ = 7.0, 6.1 Hz, $^4J_{H-H}$ = 0.9 Hz, py-H5), 5.44 (d, 1H, $^3J_{H-H}$ = 8.7 Hz, py-H3), 4.35 (dddd, 1H, $^3J_{P-H}$ = 26.6 Hz, $^3J_{H-H}$ = 11.7 Hz, $^3J_{H-H}$ = 4.6 Hz, $^3J_{P-H}$ = 4.6 Hz, Ir−C−H), 2.42 (t, 1H, $^3J_{H-H,\ trans} = {}^2J_{H-H,\ gem}$ = 9.8 Hz, NCH_2), 1.89−1.25 (m, 5H, $(CH_2)_3$), −14.81 (t, 1H, $^2J_{P-H}$ = 13.0 Hz); ^{31}P NMR (CD_2Cl_2, 298 K) 14.70, 4.02, $^2J_{P-P}$ = 339.1 Hz. FTIR (CD_2Cl_2, 298 K): ν(CO) 2035 cm^{-1}. The trans analogue, **2c**, was entirely unreactive under the same conditions.

Crystal Structure Determinations of $\mathbf{3a^{Me_2CO}}$ and **2a** were reported in ref 4.

$3a^{Me_2CO}$: A pale yellow crystal of $\mathbf{3a^{Me_2CO}}$, obtained by the slow diffusion of diethyl ether into a concentrated solution of $\mathbf{3a^{Me_2CO}}$ in dichloromethane, was mounted on a Nonius Kappa diffractometer. Triclinic; $P\bar{1}$ (No. 2); a = 11.8113(4) Å; b = 12.6330(5) Å; c = 16.5025(7) Å; α = 100.210(2)°; β = 107.894(2)°; γ = 101.536(2)°; V = 2219.4(2) Å^3; Z = 2; D_{calcd} = 1.551 g/cm^3; temperature, 183 K; Mo Kα λ = 0.710 69 Å; no. reflections ($I > 3.0\sigma(I)$) = 6997; R = 0.043, Rw = 0.042; GOF = 1.34.

2b: A colorless plate of **2b**, obtained by the slow diffusion of diethyl ether into a concentrated solution of **2b** in dichloromethane, was mounted on a Nonius Kappa diffractometer. Monoclinic; $P2_1/n$ (No. 14); a = 14.4246(6) Å; b = 14.7760(6) Å; c = 22.8912(7) Å; β = 107.342°; V = 4657.2(3) Å^3; Z = 4; D_{calcd} = 1.49 g/cm^3; temperature, 183 K; Mo Kα λ = 0.710 69 Å; μ = 32.19 cm^{-1}. No. reflections ($I > 3.0\sigma(I)$) = 5722; R = 0.032, Rw = 0.034; GOF = 0.81.

2c: A colorless plate crystal of **2c**, obtained by the slow diffusion of diethyl ether into a concentrated solution of **2c** in dichloromethane, was mounted on a Nonius Kappa diffractometer. Monoclinic; $C2/c$ (No. 15); a = 49.8735(11) Å; b = 10.8667(3) Å; c = 18.3822(4) Å; β = 110.5040°; V = 9331.3(3) Å^3; Z = 8; D_{calcd} = 1.597 g/cm^3;

temperature, 296 K; Mo Kα $\lambda = 0.710\,69$ Å; $\mu = 32.19$ cm^{-1}. No. reflections ($I > 3.0\sigma(I)$) = 5981; R = 0.057, Rw = 0.039; GOF = 1.26.

Computational Details. All calculations were performed with the Gaussian 98 set of programs[28] within the framework of hybrid DFT (B3PW91).[29] The Ir atom was represented by the relativistic effective core potential (RECP) from the Stuttgart group (17 valence electrons) and its associated (8s7p6d)/[6s5p3d] basis set,[30] augmented by an *f* polarization function (α = 0.95).[31] A 6-31G(*d,p*) basis set[32] was used for all the remaining atoms. Full optimizations of geometry without any constraint were performed, followed by analytical computation of the Hessian matrix to confirm the nature of the located extrema as minima or transition states on the potential energy surface. The thermodynamic quantities, Δ*G* and Δ*S*, were computed for 298 K within the harmonic oscillator approximation as implemented in Gaussian 98. In the case of the complexes **2t** and ***cis*-2t** with PPh_3 as a model phosphine ligand (Figure 7), the 6-31G(*d,p*) basis set was restricted to the two N atoms and to the carbene C−H moiety. The rest of the C and H atoms were treated with a 6-31G basis set due to the already high computational cost (578 basis functions, 1296 primitives, and 338 electrons). For these two systems, the frequencies of the located extrema were not computed.

Conclusions

A double geminal C−H activation has been observed in the reaction of $[H_2Ir(OCMe_2)_2L_2]BF_4$ (**1**) with several 2-amino pyridines. It occurs stepwise by way of successive cyclometalation, H_2 loss, and reversible α-elimination. The activation barriers from DFT(B3PW91) calculations are low, and all intermediates are at comparable energies, in full agreement with the observed high kinetic activity and reversibility of the reactions. The flatness of the free energy surface is shown to be due to the presence of hydrides at specific positions in the catalyst intermediates and the gain or loss of solvent as well as to the stabilizing influence of the donating amino group in the final carbene complex. Several key intermediates have been characterized or trapped experimentally. Although the phosphine ligands are trans both in the reactant and in the final products, the intermediacy of a kinetic carbene complex with *cis*-phosphine ligands, suggested by the calculations, was subsequently observed experimentally in the case of pyr-$N(CH_2)_4$.

Acknowledgment. The U.S. authors thank the U.S. DOE for funding and Michael Janzen for helpful suggestions. The French authors thanks the CNRS and Ministère of National Education for financial support. The Korean authors thank KRF(2002-070-C00053). This paper was completed by R.H.C. and O.E. while visiting UC Berkeley under Dow Chemical (R.H.C., Dow Lectures in Organic Chemistry) and Miller Institute sponsorship (O.E. Miller Visiting Professor).

Supporting Information Available: CIF file for **2c**. This material is available free of charge via the Internet at http://pubs.acs.org.

JA048473J

(28) Frisch, M. J.; Trucks, G. W.; Schlegel, H. B.; Scuseria, G. E.; Robb, M. A.; Cheeseman, J. R.; Zakrzewski, V. G.: Montgomery, J. A.; Stratmann, R. E.; Burant, J. C.; Dapprich, S.; Millam, J. M.; Daniels, A. D.; Kudin, K. N.; Strain, M. C.; Farkas, O.; Tomasi, J.; Barone, V.; Cossi, M.; Cammi, R.; Mennucci, B.; Pomelli, C.; Adamo, C.; Clifford, S.; Ochterski, J.; Petersson, G. A.; Ayala, P. Y.; Cui, Q.; Morokuma, K.; Malick, D. K.; Rabuck, A. D.; Raghavachari, K.; Foresman, J. B.; Cioslowski, J.; Ortiz, J. V.; Baboul, A. G.; Stefanov, B. B.; Liu, G.; Liashenko, A.; Piskorz, P.; Komaromi, I.; Gomperts, R.; Martin, R. L.; Fox, D. J.; Keith, T.; Al-Laham, M. A.; Peng, C. Y.; Nanayakkara, A.; Gonzalez, C.; Challacombe, M.; Gill, P. M. W.; Johnson, B. G.; Chen, W.; Wong, M. W.; Andres, J. L.; Head-Gordon, M.; Replogle, E. S.; Pople, J. A. *Gaussian 98*, rev A7; Gaussian, Inc.: Pittsburgh, PA, 1998.
(29) (a) Becke, A. D. *J. Chem. Phys.* **1993**, *98*, 5648. (b) Perdew, J. P.; Wang, Y. *Phys. Rev. B* **1992**, *82*, 284.
(30) Andrae, D.; Häussermann, U.; Dolg, M.; Stoll, H.; Preuss, H. *Theor. Chim. Acta* **1990**, *77*, 123.
(31) Ehlers, A. W.; Böhme, M.; Dapprich, S.; Gobbi, A.; Höllwarth, A.; Jonas, V.; Köhler, K. F.; Stegmann, R.; Veldkamp, A.; Frenking, G. *Chem. Phys. Lett.* **1993**, *208*, 111.
(32) Hariharan, P. C.; Pople, J. A. *Theor. Chim. Acta* **1973**, *28*, 213.